

# Rheological properties of acid converted waxy maize starches in water and 90% DMSO/10% water

E.K. Chamberlain, M.A. Rao\*

*Department of Food Science and Technology, Cornell University-NYSAES, Geneva, New York, NY 14456-0462, USA*

Received 7 January 1999; received in revised form 19 April 1999; accepted 19 April 1999

## Abstract

Rheological properties of acid-converted Amioca starches in 90% dimethyl sulfoxide (DMSO)/10% water and 100% water were examined. Rheological flow data was described using Cross and Carreau models while zero-shear viscosities were found for starches that had been acid modified at least 25 min, apparent yield stresses were exhibited by unconverted Amioca starches. Dynamic rheological tests showed that the acid modified starch dispersions behaved like Newtonian liquid-like solutions, while unconverted Amioca starches behaved like weak gels. The Cox–Merz rule was followed by starches that had been acid modified for at least 45 min. The reduction in molecule size of acid converted starches (+45 min) allowed the Cox–Merz rule to hold as opposed to the highly branched Amioca and 25 min acid converted starches which showed apparent viscosity higher than complex viscosity. © 1999 Elsevier Science Ltd. All rights reserved.

**Keywords:** Amioca starches; Cox–Merz rule; Dimethyl sulfoxide

## Nomenclature

DMSO	dimethyl sulfoxide
$\dot{\gamma}$	shear rate, $s^{-1}$
$\eta_a$	apparent viscosity, Pa s
$\eta_0$	zero-shear viscosity, Pa s
$\eta_\infty$	infinite-shear viscosity, Pa s
$\eta^*$	complex viscosity, Pa s
$\alpha_c$	Cross model time constant, $s^m$
$\lambda_c$	Carreau model time constant, s
$m$	Cross model dimensionless constant
$N$	Carreau model dimensionless constant
$\omega$	frequency, $rad\ s^{-1}$
$G'$	storage modulus, Pa
$G''$	loss modulus, Pa
$M0$	power law constant
$M1$	power law exponent
$\sigma_y$	yield stress, Pa
$\chi^2$	chi square, $\chi^2 = \sum_i^N ((y_i - f(x_i))/\sigma_i)^2$ , where
$y_i$	actual value
$x_i$	calculated value
$\sigma_i$	weight

## 1. Introduction

Starch is widely used in the food industry to thicken the continuous phase of fluid foods. The characteristics of starch dispersions are determined in order to understand fluid flow and processing parameters. The ability of starch to thicken fluid food depends on their modifications and their solubility. Acid modified starch, for example, tends to have a lower solution viscosity than the same starch that is unmodified. In addition, aggregates, or clusters of granules, will significantly affect the viscosity of starch dispersions.

Starch occurs in the form of partially crystalline, birefringent granules which consist of two chemically identical components: the linear  $\alpha$  – (1 → 4) glycosidically linked amylose and the dendroidically branched amylopectin with  $\alpha$  – (1 → 6) glycosidic bonds forming the branching points (Aberle, Burchard, Vorwerk & Radosta, 1994). Amylopectin is one of the largest molecules in nature and it plays a significant role in dictating the functional properties of starch. In order to determine the properties of the individual macromolecules, the highly organized granule has to be completely broken down to obtain a molecularly dispersed solution. Because starches are high in molecular weight, difficult to dissolve and tend to aggregate, functional properties are difficult to measure in neutral aqueous solution (Fishman, Rodriguez & Chau, 1996). Although starch is

\* Corresponding author. Tel.: + 1-315-787-2266; fax: + 1-315-787-2284.

E-mail address: mar2@cornell.edu (M.A. Rao)

a widely used polysaccharide, its physical behavior in solution is not sufficiently understood.

The inter-chain hydrogen bonding that gives the cold water insolubility of starch must be broken in order to effectively utilize the rheological properties of starch dispersions. Usually this is done with thermal energy during heating in water; however, starch will gelatinize at low temperatures in solutions of alkali, urea, dimethyl sulfoxide (DMSO) and other reagents that disrupt hydrogen bonds (Galliard & Bowler, 1987). Complete solubilization of cereal starches typically requires high temperatures and/or high pH that can result in molecular size reduction due to degradation or depolymerization, oxidation or high molar mass due to incomplete disassociation or aggregation (Yokoyama, Renner-Nantz & Shoemaker, 1998). Alternatively, dimethyl sulfoxide (DMSO) or aqueous DMSO solutions have been used to solubilize starches before characterizing them using nuclear magnetic resonance (NMR) and gel permeation chromatography (GPC).

DMSO is a powerful hydrogen bond acceptor and works by breaking associative hydrogen bonds in the polysaccharide and in water (Cooreman, van Rensburg & Delcour, 1995). Small amounts of water tend to enhance the solubilization of starch in DMSO. The water–DMSO solvent system has been used extensively as a dispersing and solubilizing agent for starch (Leach & Schoch, 1962; Banks & Greenwood, 1967; Dintzis & Tobin, 1969; Jordan & Brant, 1980; Jackson, 1991; Cooreman et al., 1995; Dintzis, Bagley & Felker, 1995; Carriere, 1998). DMSO disperses starch because both of the hydroxyl groups involved in intermolecular hydrogen bonds can become complexed to DMSO anions. A small amount of water is necessary to temporarily prevent DMSO from swelling the molecules on the surface of the starch granule as swelling would prevent DMSO from penetrating the entire granule (Jackson, 1991).

Rheology is the study of the manner in which materials respond to applied stress or strain (Steffe, 1996). The rheological response of a material depends on its molecular interactions. The Cross and Carreau models (Eqs. (1) and (2)) have been widely used to describe systems that show shear-thinning rheological behavior with a zero-shear rate viscosity at low shear rates, followed by a power law region and infinite shear rate viscosity at high shear rates.

$$\eta_a = \eta_\infty + \left( \frac{\eta_0 - \eta_\infty}{1 + \alpha_c \dot{\gamma}^m} \right) \quad (1)$$

and

$$\eta_a = \eta_\infty + \left( \frac{\eta_0 - \eta_\infty}{[1 + (\lambda_c \dot{\gamma})^2]^N} \right) \quad (2)$$

where  $\dot{\gamma}$  is the shear rate ( $s^{-1}$ ),  $\eta_a$  the apparent viscosity (Pa s),  $\eta_0$  the zero-shear rate viscosity (Pa s),  $\eta_\infty$  the infinite-shear rate viscosity (Pa s),  $\alpha_c$  ( $s^m$ ) and  $\lambda_c$  (s) are time constants, and  $m$  and  $N$  are dimensionless constants. The

constant  $\alpha$  is expressed by the ratio  $k_1/k_0$ , where  $k_0 + k_1 \dot{\gamma}^n$  is the rate constant for the rupture of linkages. A high value of  $\alpha_c$  implies a relatively large shear dependent contribution to structural breakdown (Cross, 1965). The exponents  $m$  and  $N$  are related to the power law exponent  $n$  (flow behavior index) (Lopes da Silva, 1994). Newtonian fluids have  $N = 0$  and  $m = 0$ , while fluids that exhibit shear thinning have small ( $<1$ ), positive exponents. The time constants  $\alpha_c$  and  $\lambda_c$  have the dimensions of time and are related to the onset of shear thinning. The time constant of the Cross model was shown to be in good agreement with the relaxation times obtained from stress relaxation measurements (Cross, 1979). The onset of shear thinning behavior has been found to correspond to the largest relaxation time of the solution (Chauveteau, 1982). This relaxation time was similar to the Carreau time constant at low concentrations of xanthan gum dispersions studied (Chauveteau, 1982).

Most polysaccharides exhibit similar viscosity-shear rate behavior due to their random and continuously fluctuating conformation in solution, where intermolecular interactions are typically non-specific physical entanglements (Lopes da Silva, 1994). At low shear rates, forced disentanglement is balanced by formation of new entanglements between different chains which corresponds to the zero-shear viscosity value,  $\eta_0$ . At higher values of shear rate, the rate of disentanglement exceeds that of entanglement formation; hence, the viscosity decreases and shear thinning behavior is observed (Cross, 1965).

The Cross and Carreau models have been tested for use with high-methoxyl pectin, locust bean gum, and mixtures of the two (Lopes da Silva, Gonçalves & Rao, 1992). Three parameter models were applied (assuming  $\eta_\infty \approx 0$ ) to the data and both models fit the apparent viscosity-shear rate data well. Originally, Abdel-Khalik, Hassager and Bird (1974) concluded for polymer melts that they could approximate  $\eta_\infty \approx 0$  as its contribution to the Carreau model was negligible. Lopes da Silva et al. (1992) found that the Cross model provided a slightly better fit, while the Carreau model was adept at predicting zero-shear rate viscosity values closer to experimental data.

Yield stress is defined as the minimum shear stress required to initiate flow (Steffe, 1996). The existence of a yield stress is a topic of continued debate. Barnes and Walters (1985) have argued that everything flows given sufficient time or very sensitive measuring equipment. However, the engineering reality of yield stress may have a strong impact on process parameters (e.g. moving a material along a pipe or pouring a liquid from a bottle). There are a number of methods for determining yield stress including extrapolating the shear stress vs. shear rate curve back to the shear stress intercept at zero shear rate (Steffe, 1996); values of yield stress obtained by extrapolation will depend on the flow model used (Rao & Cooley, 1983). In addition, the extrapolation is unreal in a sense, because experiments performed at progressively lower and lower strain rates

results in an asymptotic behavior towards the origin (Ross-Murphy, 1984). However, the values extrapolated from the plots will likely correlate well with practical material properties.

Controlled stress rheometers can be used to determine the viscoelastic properties of fluids and dynamic rheological information can be used to characterize or classify a dispersion. The four most common classifications are that of a dilute solution or Newtonian liquid-like solution, an entanglement network system (or a concentrated solution), a weak gel and a strong gel. A dilute solution or Newtonian liquid-like solution shows  $G''$  larger than  $G'$  over the entire frequency range, yet the moduli approach each other at higher frequencies (Steffe, 1996). The entanglement network system shows  $G''$  and  $G'$  curves intersecting at the middle of the frequency range indicating a clear tendency for more solid-like behavior at higher frequencies (Steffe, 1996). Weak gels have  $G'$  higher than  $G''$  with the moduli almost parallel to each other. Strong gels also have  $G'$  higher than  $G''$ ; however,  $G'$  has a slope of  $\approx 0$  and  $G''$  displays a minimum at intermediate frequencies (Clark & Ross-Murphy, 1987).

Cox and Merz (1958) proposed an empirical correlation between dynamic and steady shear rheological data at equal values of frequency ( $\omega$ , rad s) and shear rate ( $\dot{\gamma}$ , s<sup>-1</sup>):

$$|\eta^*| = \eta_a|_{\omega=\dot{\gamma}} \quad (3)$$

where  $\eta^*$  is the complex viscosity (Pa s) and  $\eta_a$  the apparent viscosity (Pa s). The Cox–Merz rule is an empirical relation that equates complex viscosity measured with oscillatory rheometry to shear viscosity measured in shear flow, where angular frequency is taken as the shear rate in the oscillation case (Foreman, Klinger & Wolkowicz, 1996). Using this method, the effective strain rate can be extended to over 100 s<sup>-1</sup> as frequencies over 100 rad s<sup>-1</sup> are easily measured. Dynamic rheological properties ( $G'$ ,  $G''$  and  $\eta^*$ ) can be used in comparison with steady shear rheological properties to provide insight on the structure of the sample (Da Silva, Oliveira & Rao, 1998).

The importance of the Cox–Merz rule is that it relates linear and non-linear viscoelastic properties. Therefore, shear viscosity information can be derived when only linear viscoelastic data are available and vice versa (Kulicke & Porter, 1980). Kulicke and Porter (1980) noted that good agreement with the Cox–Merz rule has been found for several synthetic polymers. Lopes da Silva and Rao (1992) found that the Cox–Merz rule was applicable for several synthetic and biopolymer dispersions, but not for biopolymer dispersions with either hyperentanglements (i.e. high density entanglements) or aggregates.

The objective of this study was to examine the rheological behavior of waxy maize starch (Amioca) at various acid conversion levels (i.e. different molecular weights) in two solvents: water and 90% DMSO/10% water. Amioca starch

was chosen because it is  $\sim 98\%$  amylopectin and allows for the characterization of the one macromolecule.

## 2. Materials and methods

### 2.1. Acid hydrolysis of starch

Waxy maize starch was reduced in molecular weight by acid hydrolysis. A 33% w/v slurry of Amioca (National Starch, Bridgewater, NJ) and 0.5N HCl was heated to 50°C with gentle mixing in a rotovap (Büchi, Switzerland) for 25, 45, or 90 min. The slurry was removed from the heat and neutralized with 1.0N NaOH. The starch dispersion was then washed and filtered with a Buchner funnel fitted with #54 hardened Whatman filter paper. Filter cakes of starch were placed in a thin layer in a stainless steel pan and allowed to air dry for  $\sim 3$  days. The filter cakes were then ground into a powder in a mortar with a pestle.

### 2.2. Starch dispersed in water

An appropriate amount of starch (0, 25, 45 and 90 min acid converted Amioca) was weighed out and added to water to make an 8% (dry weight) w/v starch dispersion. The dispersion was heated in a rotating (77 rpm) rotovap (Büchi, Switzerland) with water bath temperature set to 95°C. The temperature of the dispersion was monitored with a thermocouple. Heating continued until the dispersion reached 85°C. The dispersion was removed from the rotovap and the flask was fitted with a glass stopper. The flask was then quickly transferred to a hot oil bath set at 90°C. Heating was continued for 5 min and then the dispersion was brought to 50°C in a second oil bath and held for 20 min. Amylopectin does not retrograde as readily as amylose, but as a precaution samples were held at 50°C to avoid potential retrogradation. Samples were heated for only 5 min to exaggerate the effect of aggregation that occurs with water dispersed starch samples. Samples were then transferred to the rheometer which was programmed to wait until the plate temperature reached 20°C.

### 2.3. Starch dispersed in 90% DMSO/10% water

A 100 ml volumetric flask was partially filled with DMSO and 10 ml of distilled/deionized water was added. The mixture was allowed to come to room temperature and the remaining volume in the flask was filled with DMSO. An appropriate amount of starch (0, 25, 45 and 90 min acid converted Amioca) was weighed out and added to this 90% DMSO/10% water mixture to make an 8% (dry weight) w/v starch dispersion. The dispersion was stirred with a magnetic stir bar on a stir plate overnight ( $\sim 18$  h). The dispersion went from opaque to transparent within a few hours (time was dependent on the starch conversion level); therefore, no heat was necessary to dissolve the

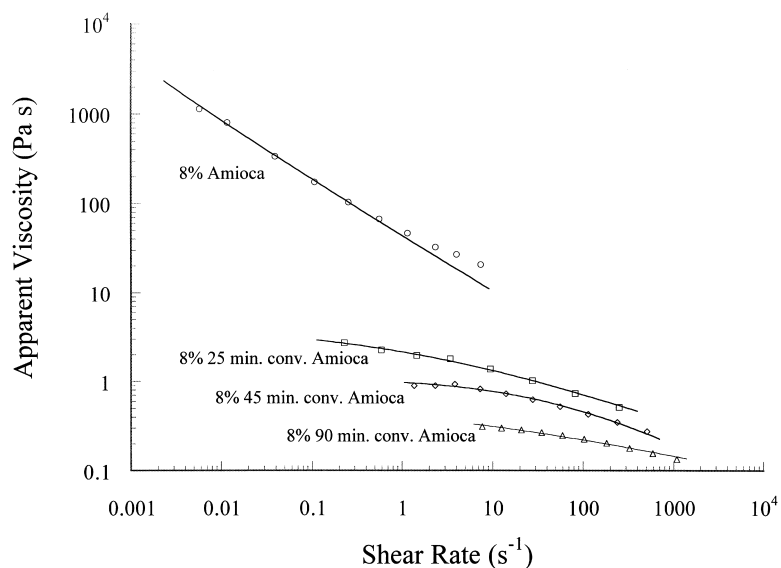


Fig. 1. Shear rate vs. apparent viscosity curves of different acid converted waxy maize starches in 90% DMSO/10% water; lines are predicted values of Cross model.

starch. Samples were checked with a light microscope and no residual aggregates were found.

#### 2.4. Rheology: flow and dynamic tests

Starch dispersions were characterized for their rheological properties using steady shear and dynamic oscillatory measurements. All rheological measurements were conducted on a controlled stress Carri-Med CSL<sup>2</sup> 100 (TA Instruments, New Castle, DE). Sample size was maintained constant using a pipette equipped with a truncated tip to reduce shearing effects.

Flow tests were performed with an anodized aluminum

cone (6 cm diameter, 2° angle) and plate arrangement. A stainless steel solvent trap was used to limit the amount of moisture evaporation. The gap was set according to the truncation of the cone as specified by the rheometer manufacturer. Shear stress was increased logarithmically in a stepped ramp mode. Approximately 50 ascending and descending points were each taken during 1 min intervals until measurements were consecutive for five points within 2% tolerance limits. Flow tests were run at 20°C for samples and plots were made of the shear rate vs. apparent viscosity and the shear rate vs. shear stress. Plots of the log shear rate vs. log apparent viscosity were also made to determine zero-shear viscosities.

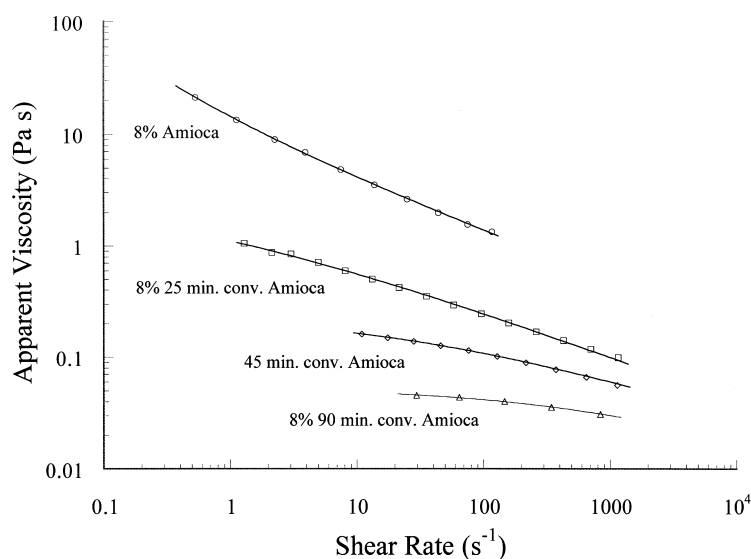


Fig. 2. Shear rate vs. apparent viscosity curves of different acid converted waxy maize starches heated in water for 5 min at 85°C; lines are predicted values of Cross model.

Table 1

Cross model parameters for 8% waxy maize starch dispersions in various solvent systems (n/a denotes not applicable)

	$\eta_0$ (Pa s)	$\alpha_c$ (s <sup>m</sup> )	$m$	$\sigma_y$	$R^2$	$\chi^2$
<i>Water</i>						
Amioca	520	49	0.45	4.0	1.0	0.39
25 min acid conv.	2.9	1.6	0.41	n/a	1.0	0.01
45 min acid conv.	0.28	0.30	0.36	n/a	1.0	0.00
90 min acid conv.	0.05	0.03	0.45	n/a	0.99	0.00
<i>90% DMSO/10% water</i>						
Amioca	5700	140	0.61	2.4	1.0	31000
25 min acid conv.	4.2	0.95	0.36	n/a	0.99	0.16
45 min acid conv.	1.1	0.13	0.52	n/a	0.99	0.03
90 min acid conv.	0.37	0.06	0.47	n/a	1.0	0.00

Dynamic rheological tests were performed with an anodized aluminum cone and plate geometry (6 cm diameter, 2° angle). A stainless steel solvent trap was used to limit effects due to moisture evaporation. First, torque sweeps were run to determine the linear viscoelastic region of the samples. It was determined that at between 1 and 8 Hz and 3–4% strain all samples were within the linear viscoelastic domain. Frequency sweeps were performed, to determine the values of  $G'$ ,  $G''$ , and  $\eta^*$  as a function of frequency, over the frequency range  $\omega = 0.1$ –100 rad s<sup>-1</sup>.

### 3. Results and discussion

#### 3.1. Steady shear data

Starch samples that had been acid converted for 25 min or longer displayed zero-shear viscosities. The Amioca samples (not subjected to acid conversion) exhibited a yield stress. The general trend exhibited by the starches in all solvent systems was that the apparent viscosity values decreased with increasing time of acid conversion. The apparent viscosity of acid converted starches dispersed in water was on the order of one decade lower than the apparent viscosity of acid converted starches dissolved in 90% DMSO/10% water (Figs. 1 and 2).

The flow curves of the acid converted starches were fitted with the Cross and Carreau models as the curves exhibited a

Table 2

Carreau model parameters for 8% waxy maize starch dispersions in various solvent systems

	$\eta_0$ (Pa s)	$\lambda_c$ (s <sup>m</sup> )	$N$	$R^2$	$\chi^2$
<i>Water</i>					
25 min acid conv.	1.2	0.86	0.18	1.0	0.01
45 min acid conv.	0.16	0.06	0.13	1.0	0.00
90 min acid conv.	0.05	0.05	0.06	0.96	0.00
<i>90% DMSO/10% water</i>					
25 min acid conv.	2.9	3.7	0.11	0.99	0.32
45 min acid conv.	0.94	0.16	0.13	1.0	0.01
90 min acid conv.	0.35	0.14	0.09	0.98	0.00

typical shear-thinning behavior with a zero-shear rate viscosity followed by a power law behavior (Figs. 1 and 2). The Carreau model was first applied to polymer melts to determine their viscosity functions from which normal stress function parameters could be estimated (Abdel-Khalik et al., 1974). The Cross and Carreau models originally were fit with four parameters, including the infinite shear viscosity ( $\eta_\infty$ ). In this experiment, negative values were determined for  $\eta_\infty$ , most likely due to the lack of data at high shear rates in the region of the limiting viscosity. The problem encountered was similar to that found with pectin and locust bean gum solutions (Lopes da Silva et al., 1992). Because  $\eta_a \gg \eta_\infty$  the Cross and Carreau models were used with only three adjustable parameters (i.e. assuming  $\eta_\infty \approx 0$ ). Results are shown in Tables 1 and 2.

The Cross and Carreau models showed relatively good fits with  $R^2$  values between 0.99–1.0 (Table 1) and 0.96–1.0 (Table 2), respectively. There is a large decrease in values for zero-shear viscosity ( $\eta_0$ ) between 25 and 45 min of acid conversion. Ali and Kempf (1986) tracked the changes in molecular weight, alkali fluidity number and iodine binding capacity during acid modification of a potato starch slurry. A rapid degradation of the starch was evident in the initial stages of acid treatment when the number-average molecular weight was reduced sharply in the first 0.75 h (Ali & Kempf, 1986). Longer treatment times (i.e. from 0.75–3 h) showed no considerable degradation but did show an increase in alkali fluidity. This was attributed to a possible attack on the hydrogen bonding of molecular chains which become more susceptible to acid attack (Ali & Kempf, 1986). In addition, very little starch was solubilized during acid modification in the work of Ali and Kempf (1986). It is likely that a similar situation occurred during the acid modification of waxy maize starch. The time constants ( $\alpha_c$ ) are larger for the water system than the DMSO/water systems (with one exception of 8% 90 min acid converted Amioca in 90% DMSO/10% water). This is likely due to the aggregates present in the water system as the dispersion was heated for only 5 min and starch granule remnants were still visible via light microscopy.

The two native Amioca samples displayed an upswing in apparent viscosity at low shear rates which is indicative of an apparent yield stress (Poslinski, Ryan, Gupta, Seshadri & Frechette, 1988; Fang, Tiu, Wu, & Dong, 1994; Rayment, Ross-Murphy & Ellis, 1995; Rao & Tattiyakul, 1999). A plot was generated of shear stress vs. shear rate to more clearly see the apparent yield stress (Fig. 3). The apparent yield stress, or a finite stress required to achieve flow, was estimated using the Herschel–Bulkley model Eq. (4), Casson model Eq. (5) and a modified Cross model (Rayment Ross-Murphy & Ellis, 1998) Eq. (6).

The Herschel–Bulkley model is defined as:

$$\sigma = K(\dot{\gamma})^n + \sigma_y \quad (4)$$

where  $K$  is the consistency coefficient,  $n$  the flow behavior

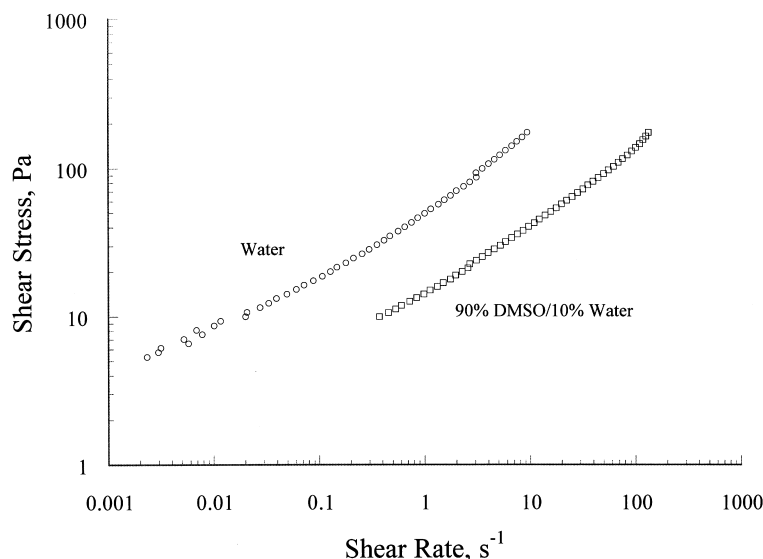


Fig. 3. Plot of shear stress vs. shear rate of 8% Amioca in water and in 90% DMSO/10% water.

index, and  $\sigma_y$  the yield stress. It is used for many fluid foods as the Newtonian, shear-thinning, shear-thickening and Bingham plastic behavior may be considered as special cases (Steffe, 1996). Water dispersed starch samples showed a 7.8 Pa yield stress while 90% DMSO dispersed starch samples showed a 6.0 Pa yield stress.

The model proposed by Casson (1959) to describe the flow of viscoplastic fluids with a yield stress is yet another general relationship for non-Newtonian fluids that has been applied to blood and food products (Macosko, 1994) and is defined as:

$$\sigma^{0.5} = \sigma_y^{0.5} + (\eta_\infty \dot{\gamma})^{0.5} \quad (5)$$

where  $\sigma_y$  is the Casson yield stress. Typically, the Casson model is used when interpreting chocolate flow data and it has been adopted as the official method by the International Office of Cocoa and Chocolate (Rao, 1995). In addition, the Casson model has also been applied to other food systems like tomato paste (Rao and Cooley, 1992). The Casson equation has also been modified by altering the exponent  $m = 0.5$ , and in this study, the exponent used was  $m = 0.25$ . The water dispersed starch (2.01 Pa) had a slightly higher yield stress than the 90% DMSO dispersed starch (1.85 Pa) system.

A modified Cross equation was also used to determine apparent yield stress values (Rayment et al., 1998):

$$\eta_a = \eta_\infty + \left( \frac{\eta_0 - \eta_\infty}{1 + \alpha_c \dot{\gamma}^m} \right) + \frac{\sigma_y}{\dot{\gamma}} \quad (6)$$

In order to obtain an apparent yield stress value,  $\sigma_y$ , the data were extrapolated to zero-shear rate using a Levenberg–Marquardt algorithm (Table 1). As a zero-shear viscosity was not obtained on these samples, the modified Cross model was forced to make an estimate of this value. A large amount of error is associated with making such esti-

mations. Although the  $R^2$  value is high (Table 1), the regression line for the 8% Amioca sample in 90% DMSO/10% water is lower than the actual data at high shear rate values due to individual variable error (Fig. 1). The modified Cross model may not be the most appropriate model to apply in these cases, but the yield stress values that are extrapolated for the 90% DMSO/10% water (2.4 Pa) and 100% water (4.0 Pa) samples are of the same order of magnitude as those determined from the Herschel–Bulkley model (6 and 7.8 Pa, respectively) and the modified Casson model with an exponent  $m = 0.25$  (1.85 and 2.01 Pa, respectively).

### 3.2. Dynamic rheological data

Dynamic rheological characteristics of waxy maize starch (Amioca) that was acid converted (0, 25, 45 and 90 min) was examined in the two different solvents (water and 90% DMSO/10% water) at 8% starch concentration (Figs. 4 and 5). Frequency sweeps ( $0.1$ – $100 \text{ rad s}^{-1}$ ) were performed at a strain of 4% which was found, by performing torque sweeps, to be in the linear viscoelastic region of all starches examined. In addition,  $G'$  and  $G''$  vs.  $\omega$  values were fitted to the power law model:

$$y = M0 \times X^{M1} \quad (7)$$

and results are reported in Table 3.

Amioca starch behaved like a weak gel while acid converted Amioca starch dispersions displayed Newtonian liquid-like behavior (Fig. 4). The storage modulus ( $G'$ ) of native Amioca was greater than the loss modulus ( $G''$ ) and the slopes of the plotted moduli values were almost parallel to each other; however, a plateau modulus was not achieved so this sample was classified as a weak gel. An apparent transition occurred in the structure after the water dispersed starch had been acid converted for 25 min; the 25 min acid converted Amioca appeared to behave like a Newtonian

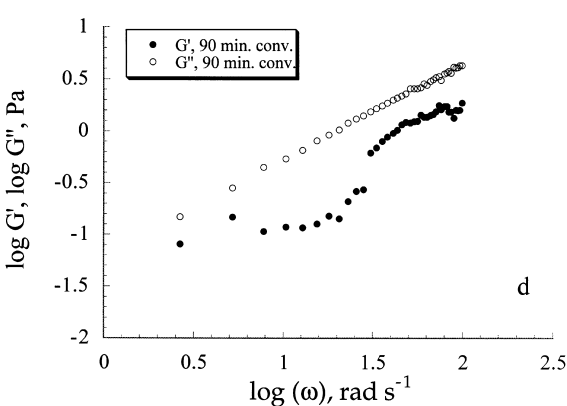
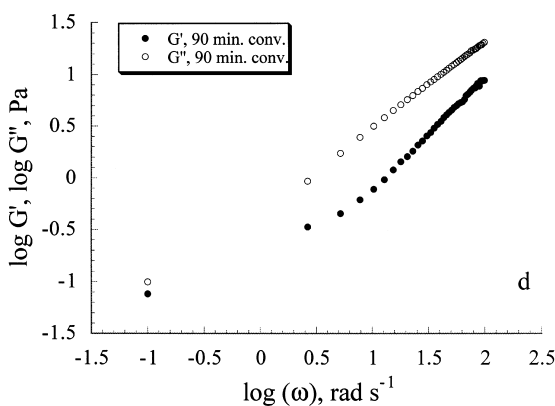
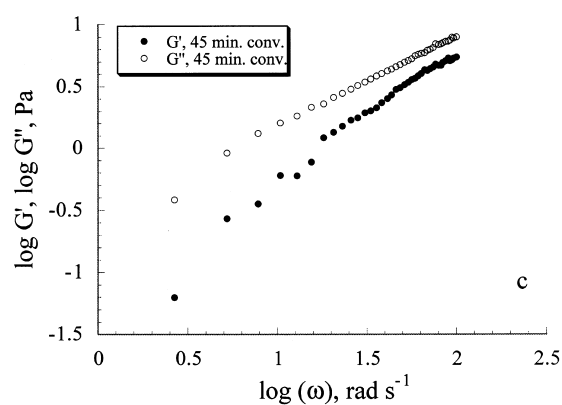
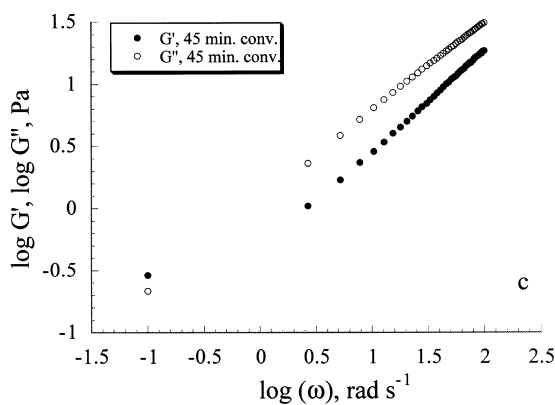
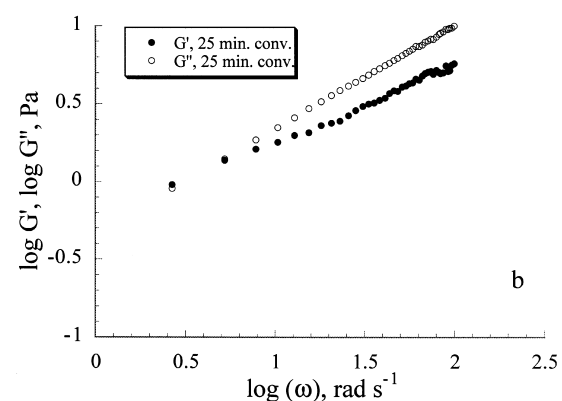
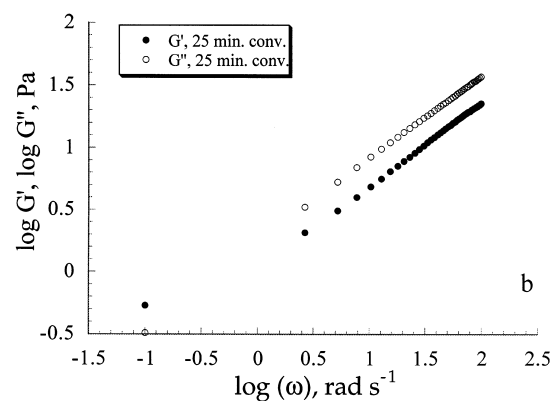
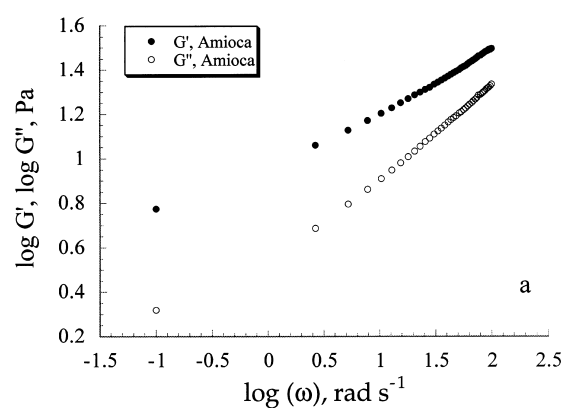
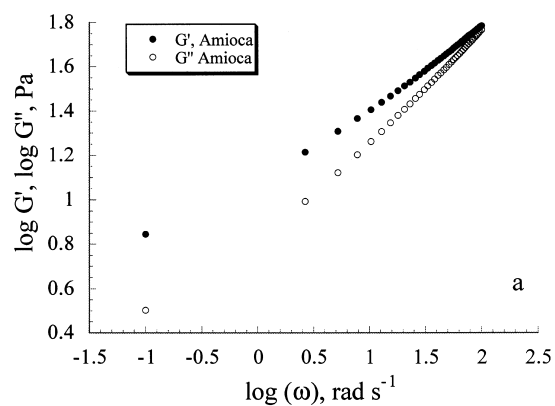


Fig. 4. (a)–(d). Comparison of magnitudes of  $G'$ ,  $G''$  of 8% acid converted waxy maize starches heated at 85°C for 5 min in water.

Fig. 5. (a)–(d). Comparison of magnitudes of  $G'$ ,  $G''$  of 8% acid converted waxy maize starches dissolved in 90% DMSO/10% water.

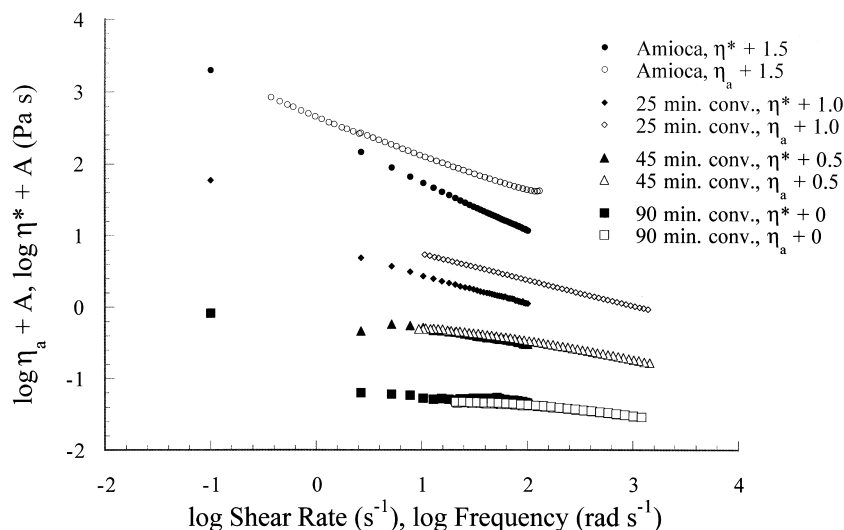


Fig. 6. Cox–Merz plot of 8% acid converted waxy maize starches heated at 85°C for 5 min in water. To avoid superposition of data, values (A) were added to  $\eta$ .

liquid-like solution and after 45 min of acid conversion, the starch system was clearly liquid-like and the storage modulus ( $G'$ ) was less than the loss modulus. The power law constant,  $M0$ , for the water based starch samples showed a transition from  $G'$  larger than  $G''$  (Amioca and 25 min acid converted starch samples) to  $G''$  larger than  $G'$  (45 and 90 min acid converted starch samples). The exponent,  $M1$ , tended to increase with increasing time of acid conversion and the  $G'$  and  $G''$   $M1$  values became more similar to each other (Table 3).

Starches dissolved in 90% DMSO/10% water mixture showed similar behavior to the water dispersed samples (Fig. 5). The Amioca sample behaved like a weak gel with  $G'$  slightly higher than  $G''$ , while the converted starches behaved like Newtonian liquid-like solutions with  $G''$  increasingly higher than  $G'$  with increased time of acid

conversion. According to Ferry (1980), if an uncross-linked polymer does not undergo entanglement coupling, then  $G''$  is always at least as large as  $G'$ . It is possible that the starches that are dissolved in DMSO do not have any apparent entanglements present. This may be due to the highly branched structure of amylopectin. The molecule may inhibit any entanglements from forming. The power law constant,  $M0$ , was larger for  $G'$  values than  $G''$  values only for 8% Amioca in the 90% DMSO/10% water solvent (Table 3). All other starch samples exhibited larger  $G''$  power law constants than  $G'$  power law constants with a decreasing trend for increasing time of acid conversion. The power law exponents were similar for  $G'$  and  $G''$  curves, with an increasing trend with increasing time of acid conversion.

### 3.3. Cox–Merz rule

The Cox–Merz rule was followed by acid-converted starches that were treated for at least 45 min. The flow and dynamic rheological data of the 45 and 90 min acid converted starches in water and 90% DMSO/10% water mixture showed overlap (Figs. 6–7). However, the native Amioca and 25 min acid converted starch deviated from the Cox–Merz rule with the complex viscosity values lower than the apparent viscosity values ( $|\eta^*| < \eta_a$ ) for each of the solvent systems used in this experiment. This could be attributed to the heterogeneous nature of starch dispersions that undergo aggregation as also seen by Da Silva et al. (1998). However, that should only hold true for the starches dispersed in water. As this behavior (i.e.  $|\eta^*| < \eta_a$ ), was also seen in 90% DMSO/10% water it seems that some other phenomenon was responsible. Perhaps this behavior was due to the highly branched structure of the Amioca and 25 min acid converted Amioca. After 45 min, the acid may

Table 3  
Power law model parameters for moduli of 8% starch dispersions

Sample	Modulus	$M0$	$M1$	$R^2$
8% Amioca-water	$G'$	9.2	0.26	0.99
	$G''$	3.8	0.37	0.99
8% 25 conv.-water	$G'$	0.84	0.39	0.97
	$G''$	0.55	0.62	1.0
8% 45 conv.-water	$G'$	0.04	1.1	0.98
	$G''$	0.25	0.76	1.0
8% 90 conv.-water	$G'$	0.05	0.71	0.91
	$G''$	0.10	0.79	0.99
8% Amioca-90/10	$G'$	12	0.33	0.99
	$G''$	6.9	0.45	1.0
8% 25 conv.-90/10	$G'$	1.4	0.59	1.0
	$G''$	1.7	0.68	1.0
8% 45 conv.-90/10	$G'$	0.73	0.68	1.0
	$G''$	1.2	0.71	1.0
8% 90 conv.-90/10	$G'$	0.18	0.81	0.99
	$G''$	0.52	0.80	1.0

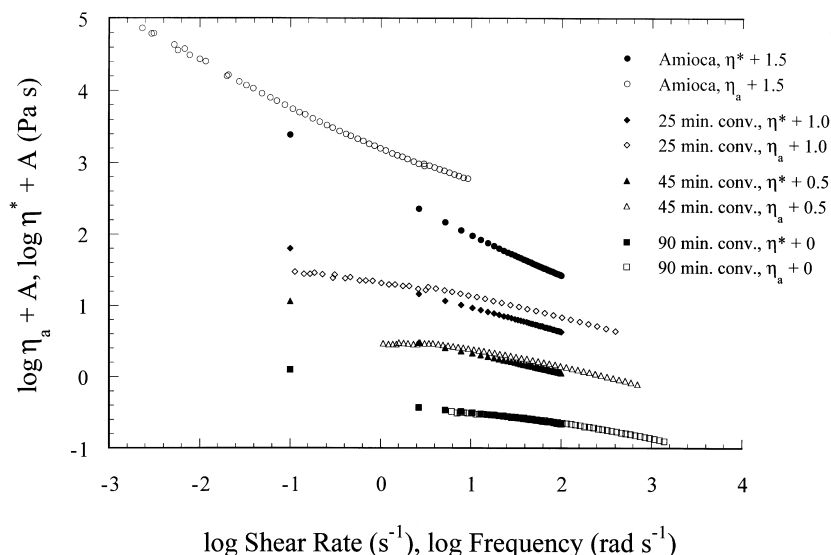


Fig. 7. Cox–Merz plot of 8% acid converted waxy maize starches in 90% DMSO/10% water. To avoid superposition of data, values (A) were added to  $\eta$ .

have cleaved enough of the amylopectin branches to allow the complex viscosity and apparent viscosity to overlap. Complex viscosity is rarely less than apparent viscosity as most departures from the Cox–Merz rule are attributed to structure decay due to the effect of the strain deformation applied to the system (i.e. low in oscillatory shear and high in steady shear). Therefore, the complex viscosity ( $\eta^*$ ) is typically higher than the apparent shear viscosity ( $\eta_a$ ) in these cases.

Lopes da Silva et al. (1992) found similar departures from the Cox–Merz rule with high-methoxyl pectin dispersions where the  $|\eta^*| < \eta_a$ . This phenomenon was considered to be due to the two-phase system of pectin micro-aggregates dispersed in solvent. This  $|\eta^*| < \eta_a$  behavior was also found in semi-dilute solutions of xanthan gum in 0.5% NaCl (Rochefort & Middleman, 1987) and for aqueous solutions of hydroxyethyl guar gum (Lapasin, Pricl & Tracanelli, 1991). Poly(ethylene-co-sodium(calcium) methylacrylic acid) melt also shows  $|\eta^*| < \eta_a$  at higher  $\dot{\gamma}$  and  $\omega$  (Kulicke & Porter, 1980). This behavior was explained to be due to ionic clusters that remained intact well above the melting point. In addition, Da Silva et al. (1998) found that the Cox–Merz rule failed with gelatinized 3–5% cross-linked waxy maize starch dispersions. They attributed this failure to the heterogeneous nature of the starch dispersions.

#### 4. Conclusion

Acid converted Amioca starch dispersions in this study could be accurately described with 3-parameter Cross and Carreau equations. The Amioca samples displayed small apparent yield stresses which were determined using Herschel–Bulkley, Casson and a modified Cross equation. Amioca in water had a slightly higher apparent yield stress

than Amioca in water. Amioca starches in both solvents behaved like weak gels; however the acid converted starches all behaved like Newtonian liquid-like solutions. The Cox–Merz rule was followed by starches that had been acid converted for at least 45 min. The Amioca starch and 25 min acid converted starch showed apparent viscosities higher than complex viscosities. This was inferred to be due to the branching found in the amylopectin molecules of Amioca and 25 min acid converted Amioca.

#### Acknowledgements

We thank Dr Judy Whaley of National Starch and Chemical Company (Bridgewater, NJ) for helpful discussions and suggestions, and USDA for NRI CGP Grant #97-35503-4493.

#### References

- Abdel-Khalik, S. I., Hassager, O., & Bird, R. B. (1974). *Polym. Engng Sci.*, 14 (12), 859–867.
- Aberle, Th., Burchard, W., Vorwerg, W., & Radosta, S. (1994). *Starch/Stärke*, 46 (9), 329–335.
- Ali, S. Z., & Kempf, W. (1986). *Starch/Stärke*, 38 (3), 83–86.
- Banks, W., & Greenwood, C. T. (1967). *Die Stärke*, 12, 394–398.
- Barnes, H. A., & Walters, K. (1985). *Rheol. Acta*, 24, 323–326.
- Carriere, C. J. (1998). *J. Polym. Sci.*, 36, 2085–2093.
- Casson, N. (1959). In C. C. Mill (Ed.), *Rheology of disperse systems*, (pp. 82). New York: Pergamon Press.
- Chauveteau, G. (1982). *J. Rheol.*, 26, 111–142.
- Clark, A. H., & Ross-Murphy, S. B. (1987). *Adv. Polym. Sci.*, 83, 57–192.
- Cooreman, F. L., van Rensburg, H., & Delcour, J. A. (1995). *J. Cereal Sci.*, 22, 251–257.
- Cox, W. P., & Merz, E. H. (1958). *J. Polym. Sci.*, 28, 619–622.
- Cross, M. M. (1979). *Rheol. Acta*, 18, 609–614.
- Cross, M. M. (1965). *J. Colloid Sci.*, 20, 417–437.

- Da Silva, P. M. S., Oliveira, J. C., & Rao, M. A. (1998). *Inter. J. Food Properties*, 1 (1), 23–34.
- Dintzis, F. R., Bagley, E. B., & Felker, F. C. (1995). *J. Rheol.*, 39 (6), 1399–1409.
- Dintzis, F. R., & Tobin, R. (1969). *Biopolymers*, 7, 581–593.
- Fang, T. N., Tiu, C., Wu, X., & Dong, S. (1994). *J. Texture Studies*, 26, 203–215.
- Ferry, J. D. (1980). *Viscoelastic properties of polymers*. 3. New York: Wiley.
- Fishman, M. L., Rodriguez, L., & Chau, H. K. (1996). *J. Agric. Food Chem.*, 44, 3182–3186.
- Foreman, J. A., Klinger, K. A., & Wolkowicz, M. (1996). *Am. Lab*, 28 (2), 19–22.
- Galliard, T., & Bowler, P. (1987). In T. Galliard (Ed.), *Starch: properties and potential*, (pp. 55). New York: Wiley.
- Jackson, D. S. (1991). *Starch/Stärke*, 43, 422–427.
- Jordan, R. C., & Brant, D. A. (1980). *Macromolecules*, 13, 491–499.
- Kulicke, W. M., & Porter, R. S. (1980). *Rheol. Acta*, 19, 601–605.
- Lapasin, R., Prici, S., & Tracanelli, P. (1991). *Carbohydr. Polym.*, 14, 411–427.
- Leach, H. W., & Schoch, T. J. (1962). *Cereal Chem.*, 39, 318–327.
- Lopes da Silva, J.A. (1994). Rheological characterization of pectin and pectin-galactomannan dispersions and gels. PhD Thesis, Universidade Catolica Portuguesa.
- Lopes da Silva, J. A., Gonçalves, M. P., & Rao, M. A. (1992). *J. Food Engng*, 18, 211–228.
- Lopes da Silva, J. A., & Rao, M. A. (1992). In M. A. Rao & J. F. Steffe (Eds.), *Viscoelastic Properties of foods*, (pp. 285). Amsterdam: Elsevier.
- Macosko, C. W. (1994). *Rheology: principles, measurements, and applications*. New York: VCH Publishers.
- Poslinski, A. J., Ryan, M. E., Gupta, R. K., Seshadri, S. G., & Frechette, F. J. (1988). *J. Rheol.*, 32 (7), 703–735.
- Rao, M. A. (1995). In M. A. Rao & S. S. H. Rizvi (Eds.), *Engineering properties of foods*, 2. (pp. 1). New York: Marcel Dekker chap. 1.
- Rao, M. A., & Cooley, H. J. (1983). *J. Food Process Engng*, 6, 159–173.
- Rao, M. A., & Cooley, H. J. (1992). *J. Texture Studies*, 23, 415–425.
- Rao, M. A., & Tattiyakul, J. (1999). *Carbohydr. Polym.*, 38, 123–132.
- Rayment, P., Ross-Murphy, S. B., & Ellis, P. R. (1998). *Carbohydr. Polym.*, 35, 55–63.
- Rayment, P., Ross-Murphy, S. B., & Ellis, P. R. (1995). *Carbohydr. Polym.*, 28, 121–130.
- Rocheffort, W. E., & Middleman, S. (1987). *J. Rheol.*, 31 (4), 337–369.
- Ross-Murphy, S. B. (1984). In H. W. -S. Chan (Ed.), *Biophysical methods in food research*, (pp. 138). Oxford: Blackwell Scientific Publications.
- Steffe, J. F. (1996). *Rheological methods in food process engineering*. 2. East Lansing, MI: Freeman Press.
- Yokoyama, W., Renner-Nantz, J. J., & Shoemaker, C. F. (1998). *Cereal Chem.*, 75 (4), 530–535.